

The Texas Medical Center Library  
**DigitalCommons@TMC**

---

UT GSBS Dissertations and Theses (Open Access)

Graduate School of Biomedical Sciences

---

12-2019

# DETERMINATION OF THYMIC EPITHELIAL CELL COMPOSITION AND PROLIFERATION DURING THE PERINATAL TO ADULT TRANSITION

Scott Casey

Follow this and additional works at: [https://digitalcommons.library.tmc.edu/utgsbs\\_dissertations](https://digitalcommons.library.tmc.edu/utgsbs_dissertations)

 Part of the [Medicine and Health Sciences Commons](#)

---

## Recommended Citation

Casey, Scott, "DETERMINATION OF THYMIC EPITHELIAL CELL COMPOSITION AND PROLIFERATION DURING THE PERINATAL TO ADULT TRANSITION" (2019). *UT GSBS Dissertations and Theses (Open Access)*. 982.

[https://digitalcommons.library.tmc.edu/utgsbs\\_dissertations/982](https://digitalcommons.library.tmc.edu/utgsbs_dissertations/982)

This Thesis (MS) is brought to you for free and open access by the Graduate School of Biomedical Sciences at DigitalCommons@TMC. It has been accepted for inclusion in UT GSBS Dissertations and Theses (Open Access) by an authorized administrator of DigitalCommons@TMC. For more information, please contact [nha.huynh@library.tmc.edu](mailto:nha.huynh@library.tmc.edu).

DETERMINATION OF THYMIC EPITHELIAL CELL COMPOSITION AND  
PROLIFERATION DURING THE PERINATAL TO ADULT TRANSITION

by

Scott Howard Casey, BA

APPROVED:

-----  
Ellen Richie, Ph.D.  
Advisory Professor

-----  
David Johnson, Ph.D.

-----  
Francesca Cole, Ph.D.

-----  
Mark Bedford, Ph.D.

-----  
Stephanie Watowich, Ph.D.

APPROVED:

-----  
Dean, The University of Texas  
MD Anderson Cancer Center UTHHealth Graduate School of Biomedical  
Sciences

DETERMINATION OF THYMIC EPITHELIAL CELL COMPOSITION AND  
PROLIFERATION DURING THE PERINATAL TO ADULT TRANSITION

A

THESIS

Presented to the Faculty of

The University of Texas

MD Anderson Cancer Center UTHealth

Graduate School of Biomedical Sciences

in Partial Fulfillment

of the Requirements

for the Degree of

MASTER OF SCIENCE

by

Scott Howard Casey, BA  
Houston, Texas

December, 2019

## ACKNOWLEDGEMENTS

I would not have made it this far without the love and support of so many people. My parents never stopped believing in me, even though I stumbled early on. Their encouragement and belief in my abilities gave me the confidence to return to school. I will also always be eternally grateful to Dr. Timothy Odell of the University of Utah. His expectation of me to be better and do more than I was gave me the drive to re-enter college. Without this amazing support network, I would never have completed my college degree or even thought of entering graduate school.

Graduate school brought new challenges, and new support. My mentor, Ellen Richie, has believed in me from the start; even when I have not. Her passion for discussing data and theories has taught me how to think of science and question the world. And the occasional (or not so occasional) reality check has kept me on track. Of course, I must thank the community of Science park as well. Michelle Bolner, who allowed me to learn what it was to be a bench scientist even as she was preparing her own defense. Katie Reeh, Nandini Singarapu, Ginny Bain, Maria Garcia, Carla Carter, Anusha Vasudev, and Encarnacion Perez have been the world's best lab mates and helped me to troubleshoot experiments that I never thought would work. And, of course without the core facilities that make Science Park so amazing, this work never would have been done. The mouse house has been essential to my research. Thank you to Meredith Spice for her witty teasing and knowledge of mice, and Debra Hollowell for teaching me so much about working with young mice. Finally, without the love and support of my best friend and partner, Kim Meyer, I would have faltered in my graduate studies long ago.

DETERMINATION OF THYMIC EPITHELIAL CELL COMPOSITION AND  
PROLIFERATION DURING THE PERINATAL TO ADULT TRANSITION

Scott Howard Casey, B.A.

Advisory Professor: Ellen Richie, Ph.D.

T-cells develop in the thymus based on signaling from multiple stromal cell types, particularly thymic epithelial cells (TECs). The thymus develops rapidly during the perinatal time period (birth – 10 days in mice) before reaching a period of homeostasis (10 days – 6 weeks). The mechanisms that initially promote and subsequently limit expansion of the TEC compartment are not known. However, previous reports from our lab suggest that the Cyclin D1-RB-E2F pathway plays a key role in regulating the perinatal to adult transition. We have previously shown that inactivation in TEC of retinoblastoma (RB) family members through deletion of RB family members or expression of cyclin D1 maintains perinatal-like TEC proliferation and continued thymus expansion. Although both cortical TEC (cTEC) and medullary TEC (mTEC) are expanded in the K5.D1 thymus, FACs analysis revealed a marked increase in a novel UEA-1<sup>int</sup> Sca-1<sup>-</sup> TEC subset, which is not readily classified as belonging to either the cTEC or mTEC lineage. In addition, low level expression of MHC class II and high-level expression of CD24 suggest that the UEA-1<sup>int</sup> Sca-1<sup>-</sup> subset contains immature TECs. Cells with this phenotype constitute a small subset of TEC in the wildtype thymus. The K5.D1 UEA-1<sup>int</sup> Sca-1<sup>-</sup> subset has a higher proliferative index compared to the wildtype subset.

Collectively, the data suggest that the UEA-1<sup>int</sup> Sca-1<sup>-</sup> subset contains TEC progenitors and that proliferation of these cells in K5.D1 TECs results in perinatal-like expansion of the TEC compartment.

## Table of Contents

<b>APPROVAL PAGE</b>	<b>i</b>
<b>TITLE PAGE</b>	<b>ii</b>
<b>ACKNOWLEDGEMENTS</b>	<b>iii</b>
<b>ABSTRACT</b>	<b>iv</b>
<b>TABLE OF CONTENTS</b>	<b>vi</b>
<b>LIST OF FIGURES</b>	<b>viii</b>
<b>LIST OF TABLES</b>	<b>ix</b>
<b>CHAPTER ONE: INTRODUCTION</b>	<b>1</b>
1.1 T cell development	1
1.2 Thymic Epithelial cells	6
1.2.1 TEC Progenitors	6
1.2.2 cTEC and mTEC subsets	9
1.3 The RB pathway regulates TEC proliferation in the adult thymus	10
1.4 T cells generated in the perinatal period have unique functional properties	12
<b>CHAPTER TWO: MATERIALS AND METHODS</b>	<b>14</b>
2.1 Mice	14
2.2 Dissociation of the thymus	14
2.3 Haematoxylin and Eosin staining	15
2.4 Immunohistochemistry	15
2.5 Flow cytometric analysis of thymus	15
<b>CHAPTER THREE: RESULTS</b>	<b>19</b>
3.1 The Cyclin D1-RB-E2F pathway regulates changes in TEC cellularity and proliferation during the perinatal to juvenile transition	19
3.2 Changes in Perinatal total thymus and TEC cellularity are not sex dependent	22

3.3 The Cyclin D1-RB-E2F pathway impacts changes in thymus architecture, TEC subset composition, and localization during the perinatal to juvenile transition	29
3.4 A phenotypically immature, cycling TEC subset is selectively expanded in the juvenile	34
<b>CHAPTER FOUR: DISCUSSION</b>	<b>45</b>
4.1 A temporal map of changes in the TEC compartment during the perinatal to juvenile transition	45
4.2 The Cyclin D1-RB-E2F pathway regulates the perinatal to juvenile transition in proliferation	47
4.3 Identification of a putative TEC progenitor population	48
4.4 Future studies	49
<b>BIBLIOGRAPHY</b>	<b>50</b>
<b>VITA</b>	<b>58</b>



## List of Figures

Figure 1. Overview of thymus structure and T cell development	2
Figure 2. Identifying TEC subsets	7
Figure 3. Total and TEC cellularity diverge in WT and K5.D1 thymuses during the perinatal to juvenile transition	20
Figure 4. Working Model	22
Figure 5. TEC proliferation in WT and K5.D1 TECs across the perinatal to juvenile transition	25
Figure 6. Changes in total thymus and TEC cellularity across the perinatal to juvenile transition are similar in male and female mice	27
Figure 7. The K5.D1 adult thymus maintains perinatal-like thymus structure	30
Figure 8. The K5.D1 adult thymus maintains a perinatal-like localization of TEC subsets	32
Figure 9. Both mTEC and cTEC subsets are expanded in the K5.D1 thymus	35
Figure 10. A novel UEA-1 <sup>int</sup> Sca-1- TEC subset is enriched in the K5.D1 thymus compared to WT thymus	39
Figure 11. K5.D1 TEC2 cells are enriched in cycling cells compared to WT TEC2 cells	41
Figure 12. Summary of results	43

**List of Tables**

Table 1. Antibodies used for flow cytometry	17
---	----

## **1 Introduction**

T cells are an essential arm of the immune response that is critical for protection from bacteria, parasites, and cancer. T cells are produced in the thymus, a bilobed organ located just above the heart. The thymus is organized into two histologically recognized regions as shown by staining tissue sections with hematoxylin and eosin (H&E). The cortex is the outer region of the thymus and stains intensely due to a high density of immature thymocytes. In contrast, the medulla stains lightly due to a smaller number of thymocytes that are relatively mature (Fig 1). During fetal development and the perinatal period, the thymus rapidly expands to produce T cells that are exported to the lymphopenic periphery. This highly proliferative stage then transitions to a brief homeostatic stage until the gradual process of age-related involution is initiated at ~7 weeks of age in the mouse. A similar process occurs in humans.

### **1.1 T cell Development**

In order to provide an effective adaptive immune system, T cells must be selected for self-restriction and self-tolerance. Self-restriction is achieved by positive selection, a process that ensures survival of thymocytes expressing T cell receptors (TCRs) with low affinity for self-peptides presented by self-major histocompatibility complex (MHC) molecules. Self-tolerance refers to the process by which T cells with high affinity TCRs for self-peptides are eliminated by apoptosis or diverted into the T regulatory (Treg) lineage.

T cell development begins with the emigration of circulating bone marrow-derived progenitors into the thymus through vessels at the corticomedullary junction (CMJ). These progenitors follow a chemokine gradient including CCL19, CCL21, and CCL25 produced by stromal cells (1-3). It is thought that this gradient attracts progenitors to a limited set of thymic stromal niches (4, 5) Once in these niches, developing thymocytes

A



B

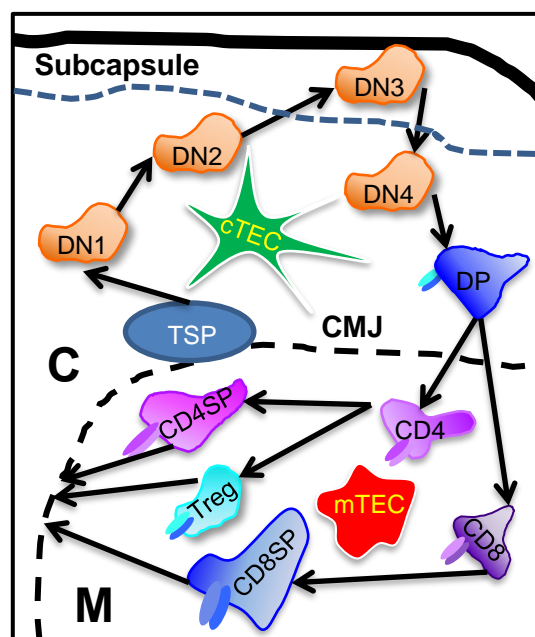


**Figure 1: Overview of thymus structure and T-Cell development**

(A) H&E stained thymus section from 6-week-old C57BL6 mouse showing cortex (dark stain) and medulla (light stain). (B) Schematic of thymocyte development and journey through the thymus. Thymocytes migrate through different microenvironmental zones. Each zone is composed of a distinct subset of stromal cells. Thymocyte subsets (TSP, DN1 – 4, DP, CD4, CD8, CD4SP, CD8SP, Treg), cTECs (green), mTECs (red). (SC) subcapsule, (C) cortex, (CMJ) cortico-medullary junction, (M) medulla (EC) endothelial cell.

go through several defined stages of development that depend on signals from cells in the thymus microenvironment, particularly thymic epithelial cells (TECs).

The major stages of T cell development are characterized by differential expression of several cell surface markers. The most immature thymocytes are negative for CD4 and CD8 and are therefore termed double negative (DN) thymocytes. The DN thymocytes are further subdivided by their expression of CD117, CD44, and CD25 molecules (7). The early CD117<sup>+</sup>CD44<sup>+</sup>CD25<sup>-</sup> DN1 cells are not yet committed to the T cell lineage, retaining the potential to differentiate into numerous cell types including B cells, natural killer (NK), and dendritic cell (DC) lineages (8). Several different signals required for T lineage commitment and continued maturation are provided by ligands and cytokines expressed by cortical TECs (cTECs). (9). For example, cTECs express the Notch ligand Delta-like 4 (DLL4) (10, 11) that activates Notch receptors leading to expression of several transcription factors which progressively commit the cell to the T cell lineage (3, 12). Notch signaling inhibits commitment to other cell fates, Loss or inactivation of the Notch signaling pathway permits DN1 thymocytes to respond to signals that mediate B-cell lineage commitment (13-15).

During the CD117<sup>+</sup>CD44<sup>+</sup>CD25<sup>+</sup> DN2 stage, thymocytes commit to T cell lineage and start the process of TCR $\beta$  rearrangement. While these cells can still be diverted from the T cell lineage, particularly to that of DC or NK cells, productive rearrangement of the TCR $\beta$  or TCR $\gamma$  chain genes restricts the cell fate potential. The germ line rearrangement of the TCR genes is driven by recombinase-activating genes (RAG). This allows the limited number of germline TCR chain genes to create a nearly unlimited array of unique receptor sequences to provide a broad diversity of antigen specificity (12, 16).

In the CD117<sup>-</sup>CD44<sup>-</sup>CD25<sup>+</sup> DN3 stage, cells that have undergone productive TCR $\beta$  rearrangement pair the TCR $\beta$  chain with the invariant pre-TCR $\alpha$  (pT $\alpha$ ) chain to

form what is known as a pre-TCR. Expression of pre-TCR on the surface of the thymocyte rescues cells from programmed cell death (17, 18). The successfully expressed pre-TCR also provides intracellular signals that allow maturation to the transient CD117<sup>+</sup>CD44<sup>+</sup>CD25<sup>-</sup> DN4 stage. This stage is marked by 8-9 rounds of proliferation and the initiation of CD4 and CD8 expression. Thymocytes that express both CD4 and CD8 are referred to as double positive (DP) (19).

Thymocytes that mature to the DP stage initiate another round of RAG-dependent gene rearrangement, this time to rearrange the TCR  $\alpha$ -chain. Productive rearrangement of the TCR $\alpha$  gene is required to generate functional TCR $\alpha$  polypeptides that pair with TCR $\beta$  polypeptides to form a functional  $\alpha\beta$ TCR. DP thymocytes undergo this rearrangement until either positive selection signals are received, which stop rearrangement, or  $\alpha$ -chain rearrangement possibilities are exhausted. DP thymocytes have a short half-life of ~3 days and undergo apoptosis if they are not rescued from cell death. Thymocytes that fail to express  $\alpha\beta$ TCRs or that express  $\alpha\beta$ TCRs that do not recognize self-peptide/MHC undergo apoptosis (20). The vast majority of DP thymocytes undergo one of these two fates. DP thymocytes that express  $\alpha\beta$ TCRs with low affinity for self-peptide/MHC complexes presented by cTECs are rescued from cell death by positive selection, and continue to differentiate (21). This stringent positive selection process ensures that thymocytes that proceed to further stages of development will only react to antigen presented by the organism's own cells. Positive selection results in downregulation of either CD4 or CD8 to become either CD4<sup>+</sup> or CD8<sup>+</sup> single positive (SP) thymocytes (21, 22) and upregulation of chemokine receptors such as CCR7, allowing SP cells to migrate into the medulla in response to chemokines produced by medullary TECs (mTECs) and dendritic cells (DCs).

In the medulla, thymocytes interact with mTECs and DCs to establish central tolerance, a process that either purges T cells that have autoreactive potential or

generates T cells that can suppress autoreactivity. The mTEC subset has the unique ability to express a wide array of tissue restricted antigens (TRAs). SP thymocytes with high affinity TCRs for TRAs expressed in the context of self-MHC by mTECs are deleted by apoptosis. In addition, mTECs transfer TRAs to DCs for cross-presentation to thymocytes, leading to additional deletion of highly autoreactive SP thymocytes. (23, 24). This negative selection process removes most, but not all, potentially autoreactive thymocytes (20). If SP thymocytes express TCRs that recognize TRAs with moderate affinity, they may not undergo apoptosis, but instead may be diverted into the T regulatory (Treg) lineage (25). Tregs in the periphery inhibit autoreactive T cells and aid in restricting the immunological response to foreign antigens providing an additional safe-guard against autoimmunity (26). SP thymocytes that escape negative selection are then ready to emigrate from the thymus to the peripheral lymphoid organs. These thymocytes follow a gradient of chemokines, such as S1P, to the thymic vasculature, where they exit the thymus and enter the peripheral T cell pool (27).

## **1.2 Thymic Epithelial Cells**

The previous description of thymocyte development demonstrates that TECs provide indispensable signals for T cell development at every stage of maturation. This section will summarize cellular and molecular features of TEC subsets in fetal and adult thymuses.

### **1.2.1 TEC Progenitors**

The thymus develops as an epithelial organ from the ventral domain of the 3<sup>rd</sup> pharyngeal pouch (PP). Fetal TEC progenitors are bipotent for both cTEC and mTEC lineages. Commitment to the cTEC or mTEC lineage is the result of complex interactions with the mesenchyme and emigrating lymphoid progenitors (28, 29). Whether these fetal-derived bipotent progenitors persist in the adult thymus is uncertain. There have

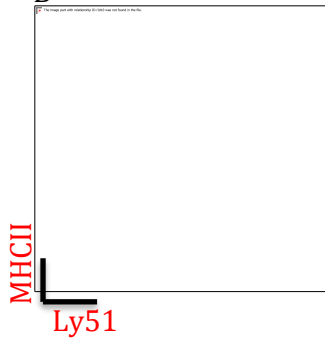


A

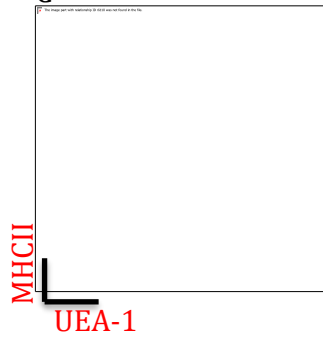


K8 K5 K14

B



C



D

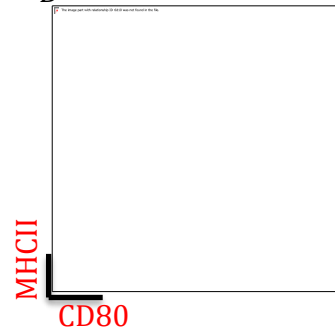


**Figure 2: Identifying TEC subsets.**

(A) Overview of TEC subsets visible by IHC including cTECs (dense green stain in cortex), K8<sup>-</sup>K5<sup>+</sup>K14<sup>+</sup> mTECs (pink cells in medulla), and K8<sup>+</sup>K5<sup>-</sup>K14<sup>-</sup> mTECs (bright green cells in medulla). (B, C, and D) FACS separation of TECS based on MHCII expression and (B) expression of Ly51, (C) binding of UEA-1, and (D) expression of CD80 in 4-week-old WT mouse thymus.

been reports from two independent groups of in vivo adult bipotent TEC progenitors; however, the populations identified by these two groups do not match each other. The Blackburn lab reported an EpCAM<sup>+</sup> Ulex Europaeus Agglutinin 1 negative (UEA-1-) Ly51<sup>+</sup> PLET1<sup>+</sup> MHCII<sup>hi</sup> TEC population that exhibited bipotent progenitor capability (30). In contrast, the Chidgey lab identified an MHCII<sup>lo</sup>  $\alpha$ 6-integrin<sup>hi</sup> Sca1<sup>hi</sup> Ly51<sup>lo</sup> TEC population that retained label (BrdU) and exhibited bipotent progenitor activity (31, 32). These populations were identified using somewhat different approaches and more research is needed to identify the bipotent progenitor population(s).

In addition to bipotent progenitors, embryonic mTEC lineage restricted progenitors have been identified. These cells are marked by their expression of the tight junction proteins claudin 3 and 4. They are located in the apical layer of the 3<sup>rd</sup> PP prior to thymus separation and give rise solely to Aire<sup>+</sup> mTECs (32, 33). While they do persist into adulthood, their progenitor potential is drastically reduced (32, 33).

### 1.2.2 cTEC and mTEC subsets

The cTEC subset has been characterized using a variety of cell surface and intracellular markers. cTECs are mostly keratin 8 negative (K8-), keratin 5 negative (K5-), and keratin 14 negative (K14-). The cTEC subset also expresses CD205, Ly51 (Fig 2B), and the thymoproteasome subunit  $\beta$ 5t. The  $\beta$ 5t subunit is the only marker of the cTEC subset implicated in their role in positive selection. The  $\beta$ 5t subunit is thought to be required for the thymoproteasome to produce self-peptides for presentation in the context of MHCII during positive selection (34). Finally, cTECs can be identified as immature or mature based on their expression of MHCII (FIG 2B). Since all of the known cTEC markers are expressed on most cTECs, it has not yet been possible to discriminate phenotypically distinct cTEC subsets.

In contrast, mTECs can be identified by a variety of markers and separated into several phenotypical and functional subpopulations. The majority of mTECs are K8<sup>-</sup> K5<sup>+</sup> K14<sup>+</sup> (Fig 2A). A smaller population is K8<sup>+</sup> K5<sup>-</sup> K14<sup>-</sup> UEA1<sup>+</sup>, is marked by a more rounded structure (Fig 2A). Like cTECs, mTECs can be separated by their expression of MHCII into canonically mature (MHCII<sup>hi</sup>) and immature (MHCII<sup>lo</sup>) TECs (Fig 2C). All mTECs are positive for UEA-1 by flow cytometric analysis (Fig 2C). The surface protein CD80 can also be used to separate mTECs into immature and mature subsets (Fig 2D). mTECs can then be further subdivided based on their expression of CD80, which positively correlates with MHCII and the mTEC maturity level.

A subset of mature mTECs has the unique ability to express a wide array of antigens that are normally restricted to specific tissues in the periphery. The transcription factor autoimmune regulator (AIRE) is essential for this ability (35, 36). In addition to expressing TRAs, mTECs transfer them to DCs for cross-presentation Reviewed in (21). TRA expression is critical for deleting self-reactive SP thymocytes. Mice and humans that lack the ability to express TRAs present with widespread autoimmunity (35, 37).

There is also a small TEC subset that is not readily identifiable as belonging to either the cTEC or mTEC lineage, because it costains for K5 and K8. These cells are located in and around the cortico-medullary junction (CMJ) (Fig 2A).

The majority of the data on TEC subsets has been gathered in young adult thymuses. Those studies that examine the make-up of the TEC compartment as a function of age typically do so either in the fetal or adult thymus or the aged, involuting thymus. This leaves a large gap in our knowledge of the development of the thymus where the perinatal thymus is concerned.

### **1.3 The RB pathway regulates TEC proliferation in adult thymus.**

There are some reports that examine the changes in TEC proliferation as a function of age from fetal to adult. Fetal and early perinatal mice thymuses have the highest proportion of cycling TECs (38). This was reported to fall off sharply with age, from ~33% of TECs cycling at the early perinatal stage to ~6% at 4 weeks of age, and drops even further to ~2% in a 10-month-old mouse (38). The mechanisms that regulate this change from a highly proliferative organ to a homeostatic one are not understood. However, our lab has obtained evidence that the Cyclin D1-RB-E2F pathway plays a role {Garfin, 2013 #54;Klug, 2000 #55;Robles, 1996 #56}.

The retinoblastoma protein (RB) is a well-documented cell cycle regulator (39-41). Unphosphorylated and monophosphorylated RB is bound to the E2F transcription factor which targets the promoter regions of target genes (42). Unphosphorylated RB recruits permanent repressive machinery to these promoter sites, inhibiting proliferation and promoting terminal differentiation (42). Growth factors trigger the upregulation of Cyclin D1, which activates and binds to cyclin dependent kinases 4 and 6 (CDK4/6). The activated CDK4/6 then monophosphorylates RB, which recruits temporary suppression machinery and prevents the cell from exiting the cell cycle (42). Additionally, the monophosphorylation primes the RB for hyperphosphorylation by Cyclin E activated CDK2 in late G1(42). The hyperphosphorylated RB releases the bound E2F transcription factor to drive S-phase entry (42).

Our lab found that expressing a keratin 5 promoter driven Cyclin D1 transgene in the TEC compartment results in continuous thymus growth (43, 44). The transgene is expressed only in the TEC compartment, and the sustained thymus growth is not because of either thymic lymphoma or thymoma development (43, 44). The K5.D1 thymus is compartmentalized into cortical and medullary regions and supports T cell development, including positive and negative selection. A later study in which we collaborated with the Sage lab showed that conditional deletion of the RB family in TECs

results in a thymus expansion phenotype similar to that of K5.D1 (45). Together, these findings strongly implicate the Cyclin D1-RB-E2F pathway in regulating TEC proliferation and thymus growth.

#### **1.4 T cells generated in the perinatal period have unique functional properties**

Newborns are uniquely vulnerable to infection, making it essential that perinatal T cells provide a strong immune response that is still self-tolerant. To fill this need, T cells produced during the perinatal period possess several unique functions. They provide a rapid, strong, innate-like response to pathogens, but this response is short-lived (46, 47). To ensure that this strong reactivity does not cause autoimmunity, Tregs produced in the perinatal thymus are highly suppressive and required to maintain suppression of autoreactivity throughout life (48). Recent reports have shown perinatal Tregs to be required to prevent peripheral T cells from responding to antigen, a state known as anergy (49). This prevents immune reactions against commensal microbes in the skin (50).

Given that the TECs are not only essential for T cell development, but are also critical for selecting a self-restricted and self-tolerant TCR repertoire, it is possible that at least some of the functional attributes of perinatal T cells are due to unique functions of the perinatal versus adult TEC compartment. Increased levels of CD5, an indicator of the combined affinity for antigen of a T cell's TCRs, on thymocyte subsets have also been reported in neonatal and young mice. This suggests that the perinatal selection process favors T cells with TCRs possessing a stronger affinity for self-peptide MHC complexes. Additionally, differences in peptide processing have recently been implicated in the unique TCR repertoire of perinatal Tregs required for suppression of autoimmunity throughout life (48).

However, there is very little information on perinatal TECs because most studies on TEC subsets are conducted in the fetal, adult, or involuting thymus. The goals of this project were 1) to determine if TEC subset composition and proliferation changes during the perinatal to adult transition and, 2) determine if the Cyclin D1-RB-E2F pathway affects TEC subset composition and proliferation during this period.

## **2 Materials and Methods**

### **2.1 Mice**

K5.Cyclin D1 mice were originally generated by C. Conti (44) and were maintained on a C57BL6/J background. C57BL6/J mice were purchased from the Jackson Laboratory (Bar Harbor, Maine), and crossed with heterozygous K5.Cyclin D1 transgenic mice. The K5.Cyclin D1 genotype was confirmed using PCR. Mice were maintained in a specific pathogen free environment in accordance with all MD Anderson Institutional Animal Care and Use Committee policies. Single cell suspensions of mouse thymuses were analyzed by flow cytometry at embryonic day 17.5 and day 0, 3, 7, 10, 14, and 28 days postnatal.

### **2.2 Dissociation of Thymus**

Thymuses were excised from the thoracic cavity, washed with 1x PBS (pH 7.0), and then trimmed of excess tissues. Cleaned thymuses were then diced into numerous small pieces and digested using a buffer of 0.52 Wunsh Units/mL Liberase TM (Roche) and 20 units/mL of DNase I (Roche) in PBS (pH 7.0). Tissues were digested in 2mL in a shaker incubator at 37C and 180 RPM for 10 minutes. Supernatant was collected into 40mL of FACS wash buffer (1x PBS pH7.0, 2% Bovine Calf Serum, 0.05M EDTA), leaving undigested tissue in the tube, and process was repeated twice more. Any undigested tissue was manually dissociated using a p1000 pipette. Collected supernatant was then centrifuged at 1500 RPM for 5 minutes. The Cell pellet was resuspended in FACS wash buffer, 5mL for wildtype adult thymuses and 10mL for adult K5.Cyclin D1 thymuses. Cell suspensions were filtered using a 0.7 um cell strainer (Falcon) and then counted on a hemocytometer using trypan blue for live/dead differentiation.



### **2.3 Haematoxylin and Eosin staining**

Fresh frozen sections were thawed to room temperature and fixed using 10% neutral buffered formaldehyde. Slides were treated with haematoxylin (Sigma) for 10 minutes and rinsed briefly in water. Haematoxylin stained slides were then treated with 1% eosin (Sigma) for 3-10 minutes and rinsed briefly with water. Stained slides were dehydrated with ethanol beginning at 70% and ending at 100% before being washed with xylene twice for 10 minutes. Cover slips were added and sealed with cytooseal (Thermo Scientific) and imaged.

### **2.4 Immunohistochemistry**

Serial sections (8-10  $\mu\text{m}$ ) from optimal cutting temperature medium (OCT) embedded tissue were air dried and fixed in cold acetone at room temperature or  $-20^{\circ}\text{C}$ . Fixed slides were washed with phosphate buffered saline (PBS) and then incubated with rat anti-mouse K8 serum overnight at room temperature. Slides were washed in PBS and then stained with optimal concentrations of rabbit anti-mouse Keratin 5 (Covance) and chicken anti-mouse Keratin 14 (Biolegend) at room temperature for 1 hour. Slides were washed and treated with appropriate secondary antibodies for 30 minutes. Cover slips were added and sealed using Prolong Gold (Invitrogen) and imaged using a Leica DMI 6000 B fluorescent microscope. Staining with secondary antibodies in the absence of primary antibody was used as a negative control.

### **2.5 Flow cytometric analysis of thymus**

Thymus cell suspensions were stained with a panel of antibodies for live or fixed staining (Table 1). Antibodies were added to  $4 \times 10^6$  cells in 100  $\mu\text{L}$  for 15 minutes in the dark at  $4^{\circ}\text{C}$ . For fixed analysis, samples were then fixed and permeabilized using a BD Biosciences fixation/permeabilization kit. Samples were centrifuged at 400 rcf for 3 minutes, and were brought to 500  $\mu\text{L}$  with FACs wash buffer for analysis using a BD

FACs Aria II cell sorter or BD Fortessa cell analyzer. Analysis was conducted on collected data using the FlowJo (version 9.4.10 – version 10.5.3) program by FlowJo (Ashland, Oregon).

<b>Antibody</b>	<b>Fluorochrome</b>	<b>Manufacturer</b>
UEA-1	FITC	Vector
$\alpha$ CD80	PE	eBioscience
Propidium Iodide		
$\alpha$ CD24	PE/Cy7	eBioscience
$\alpha$ CD11c	PerCP/Cy5.5	Tonbo
$\alpha$ EpCam	APC	Biolegend
$\alpha$ la/le	APC/Cy7	Biolegend
$\alpha$ Sca-1	Pac Blue	Biolegend
$\alpha$ CD45	BV510	Biolegend
$\alpha$ Ly51	Biotin	BD Pharmingen
Streptavidin	Qdot-605	Life Technologies
Rat IGG2a K Isotype Control	Biotin	BD Biosciences
$\alpha$ la/le	PE	Tonbo
$\alpha$ EpCam	PE/Cy7	Biolegend
$\alpha$ Sca-1	APC/Cy-7	Biolegend
Streptavidin	Qdot-655	Life Technologies
$\alpha$ Ki67	A700	eBioscience
Rat IGG2a K Iso Control	A700	eBioscience

**Table 1: Antibodies used for flow cytometry**

### 3 Results

#### 3.1 The Cyclin D1-RB-E2F pathway regulates changes in TEC cellularity and proliferation during the perinatal to juvenile transition.

As discussed in the Introduction, previous studies have implicated the Cyclin D1-RB-E2F pathway in regulating TEC proliferation (43-45). In order to determine if this pathway regulates proliferation during the perinatal period, we compared thymus and TEC cellularity changes in wildtype (WT) versus K5.D1 across the perinatal to adult transition. The WT thymus grows exponentially from birth until perinatal day 10-14 (P10-P14)(Fig 3A) when it enters a homeostatic phase that lasts for the next ~2 months (51). The cellularity of the K5.D1 thymus increases at the same exponential rate as the WT until ~P10 (Fig 3A). At this point, the K5.D1 thymus does not switch to a homeostasis program, but instead maintains exponential growth (Fig 3A). A similar pattern is seen in the TEC compartment, except that the shift in growth occurs earlier. In the WT thymus, TEC cellularity increases rapidly until ~P3-P7 (Fig 3B). By P7, K5.D1 TEC cellularity exceeds that of the WT and continues to expand at a faster rate than the WT through P28 (Fig 3B). It is important to note that WT and K5.D1 TEC cellularity diverges before the total thymus cellularity does, P7 vs P10 (Fig 3A,B). This supports TEC expansion as a key driver of thymus growth and suggests that the Cyclin D1-RB-E2F pathway is a key regulator of the shift between a proliferative program and a homeostatic one.

Based on these data, we generated a model of the regulation of the perinatal to juvenile transition. Because the increase in TEC cellularity was approximately identical in WT and K5.D1 thymuses until day 7, we propose that in the WT thymus, RB in early perinatal TECs is constitutively monophosphorylated. Based on RB's known functions, this would be expected to inhibit terminal differentiation and prime the TECs for hyperphosphorylation and entry into s-phase, resulting in a higher proportion of actively

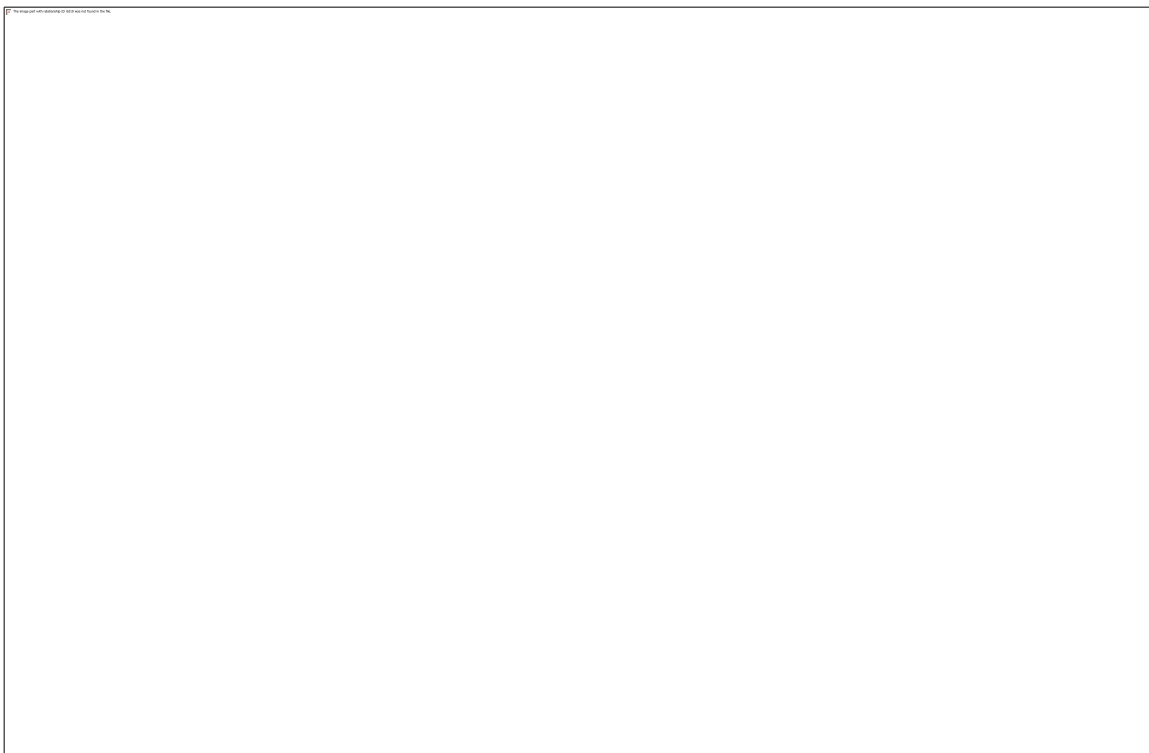


**Figure 3: Total and TEC cellularity diverge in WT and K5.D1 thymuses during the perinatal to juvenile transition**

WT (blue) and K5.D1 (red) total thymus cellularity (A) and TEC compartment cellularity (B). N-value of at least 4 mice per time point and genotype. \* $P < 0.05$ , \*\* $P < 0.01$ , \*\*\* $P < 0.0001$ , and \*\*\*\* $P < 0.00001$  using an unpaired two-tailed Student T test.

cycling cells. After the transition between P7-P14, we propose that RB in TECs is no longer constitutively monophosphorylated. Based on RB's function, this would inhibit proliferation as fewer TECs are now primed for hyperphosphorylation and a higher proportion of them are now programmed for terminal differentiation. (Fig 4). In this model expression of the K5.D1 transgene would override the switch in RB phosphorylation states.

A prediction of our model is that the frequency of proliferating TECs would decrease around day 7 in the WT thymus, and that the K5.D1 thymus will maintain a high frequency of proliferating TECs. To check the model's predictions about TEC proliferation, we quantified the percentage of Ki67 positive WT versus K5.D1 TECs across the perinatal to juvenile transition. As predicted by the model, there was a high frequency of proliferating WT TECs prior to and immediately after birth (Fig 5). The frequency of Ki67 positive TECs decreased by 3 days of age (Fig 5) in the WT thymus. In contrast to the decreased proliferation seen in WT TECs, the frequency of cycling K5.D1 TECs was identical until day 3, but after this point the K5.D1 TEC compartment maintains a high frequency of cycling cells (Fig 5). These results support the model, which predicts that constitutive monophosphorylation in TECs by ~P7 in the WT thymus to prevent unrestrained thymus growth.

### **3.2 Changes in perinatal total thymus and TEC cellularity are not sex dependent.**

There are known sexual dimorphisms in thymus involution with female mice and humans displaying a slower involution than males (51). Whether a similar sexual dimorphism exists in the perinatal to juvenile transition is currently unknown. When we separated the thymus and TEC cellularity by sex, we found no difference in the growth of the thymus or the TEC compartment based on sex in either WT or K5.D1 mice (Fig 6).



The image and all contents © 2023 are the property of the PwC

**Figure 4: Working Model**

Our proposed model for the regulation of proliferation in TECs. In this model, prior to P7 proliferation occurs without RB regulation affecting it. The transition occurs between P7 and P14. After the transition, RB regulates proliferation and must be hyper-phosphorylated to release E2F transcription factors to drive proliferation and differentiation.

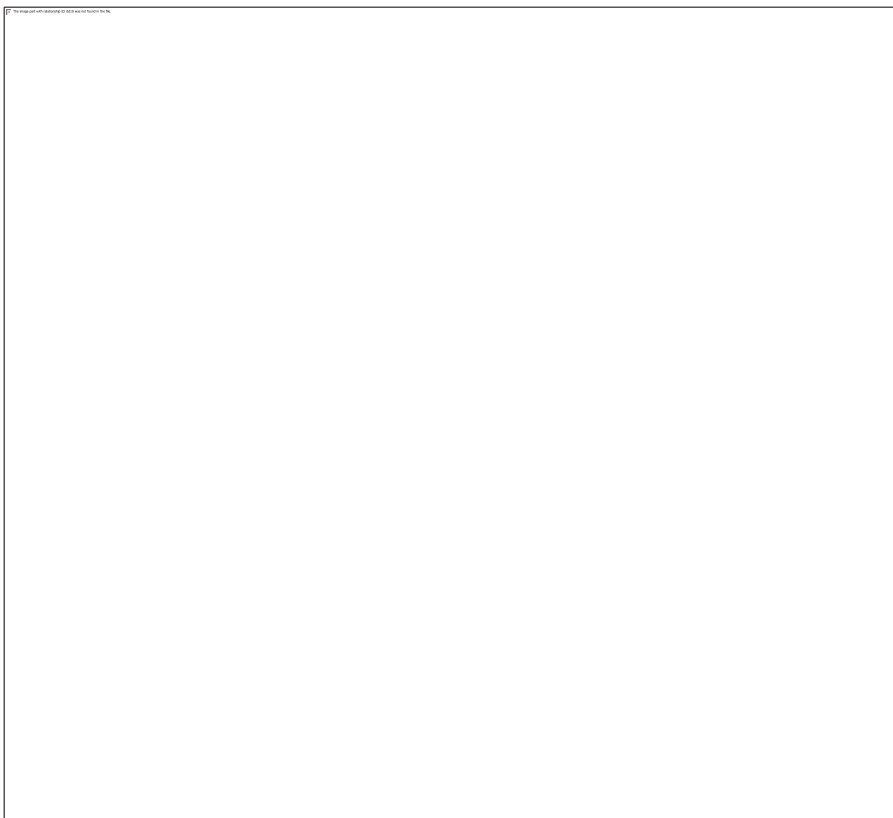


**Figure 5: TEC proliferation in WT and K5.D1 TECs across the perinatal to juvenile transition**

Percentage of TECs that are Ki67+. The % Ki67+ TECs declines in WT (blue) after P0, but is maintained in the K5.D1 (red). N-value of at least 2 mice per time point and genotype. \*P<0.05, \*\*P<0.01, \*\*\*P< 0.0001, and \*\*\*\*P< 0.00001 using an unpaired two-tailed Student T test.

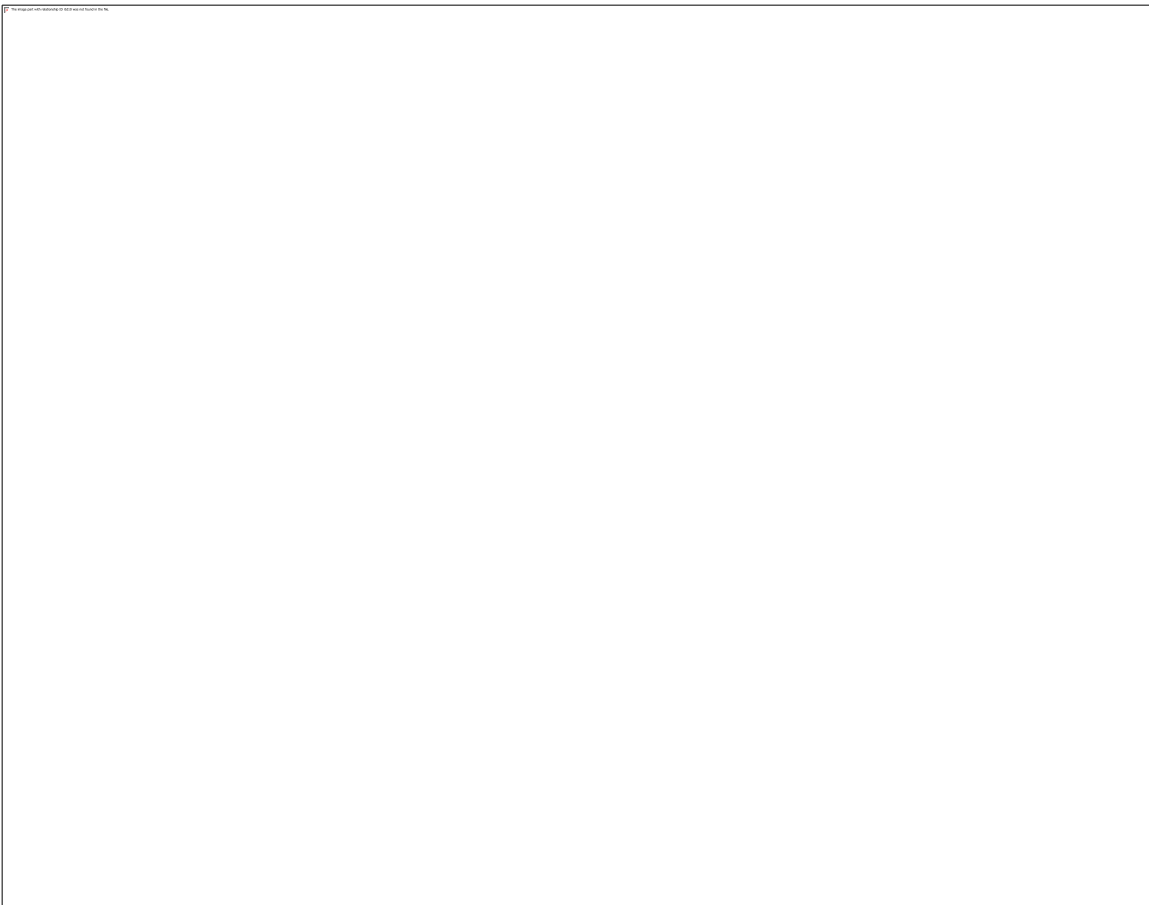


**Figure 6: Changes in total thymus and TEC cellularity across the perinatal to juvenile transition are similar in male and female mice**

(A) Sex specific total thymus cellularity in WT and K5.D1. (B) Sex specific TEC compartment Cellularity in WT and K5.D1. N-value of at least 2 mice per time point, sex, and genotype. \* $P < 0.05$ , \*\* $P < 0.01$ , \*\*\* $P < 0.0001$ , and \*\*\*\* $P < 0.00001$  using an unpaired two-tailed Student T test.

### **3.3 The Cyclin D1-RB-E2F pathway impacts changes in thymus architecture, TEC subset composition, and localization during the perinatal to juvenile transition**

The WT thymus undergoes extensive remodeling during the perinatal period, which is apparent in H&E stained thymus sections. For example, the medulla initially develops as clonally derived islets (52). During the perinatal to juvenile transition these islets coalesce into large, central medullary regions in the WT thymus (Fig 7A). In contrast, the K5.D1 maintains a large number of small medullary regions across the perinatal to juvenile transition (Fig 7B).

Changes in localization of TEC subsets during the perinatal to juvenile transition are apparent by Immunohistochemistry (IHC) analysis of thymus sections stained with fluorescence-tagged Abs to keratins. The cTEC compartment is K8+K5-K14<sup>-</sup>, while the major mTEC subset is K8-K5+K14<sup>+</sup> (Fig 8A)(53). As with the medullary structure seen by histological analysis (Fig 7A,B), K8-K5+K14<sup>+</sup> mTECs are present throughout the wildtype perinatal thymus in small islets (Fig 8A), but are concentrated into cohesive medullary regions in the adult thymus (Fig 8B). In the perinatal K5.D1 thymus, these K8-K5+K14<sup>+</sup> cells are also localized in widespread medullary islets (Fig 8A), and the adult K5.D1 thymus maintains the widespread distribution of K8-K5+K14<sup>+</sup> islets seen in the perinatal (Fig 8B). There is also a rare subset of putative K8+K5+K14<sup>-</sup> TEC progenitors that is found at the CMJ and sporadically in the cortex of the WT adult thymus (Fig 8B) (53, 54). The WT and K5.D1 perinatal thymuses are enriched for this subset (Fig 8A,C). In contrast to the distribution of these K8+K5<sup>+</sup> cells in the adult WT thymus, the K5.D1 thymus exhibits a perinatal like distribution and prevalence of this putative progenitor population.

The structural and localization differences between the perinatal and adult WT are reflected in the composition of the TEC compartment across the perinatal to juvenile transition. At birth mTECs and cTECs number  $\sim 1 \times 10^4$  cells (Fig 9A,B). The cTEC

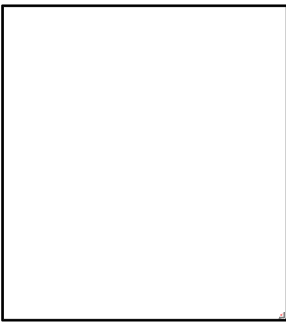
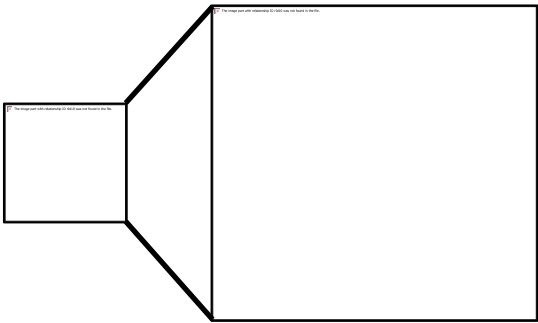
Day 3

6 Weeks

A

B

WT



C

D

K5.D1

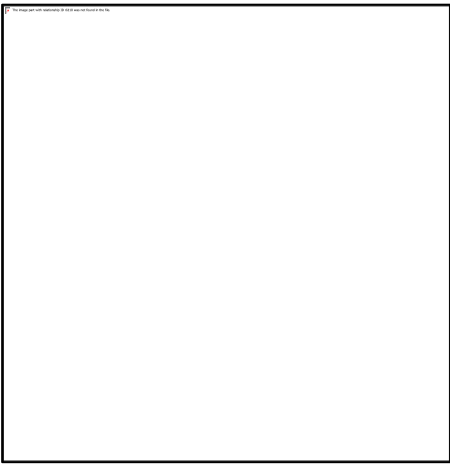
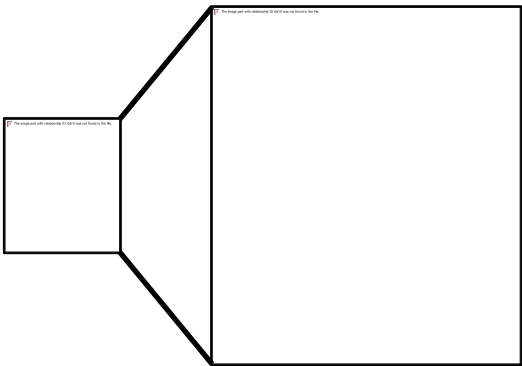




**Figure 7: The K5.D1 adult thymus maintains perinatal-like thymus structure**

Representative H&E stained thymus sections showing small, dispersed medullary islets in P3 WT (A) and K5.D1 (C). Medulla has coalesced by 6 weeks in the WT (B), but the 6-week K5.D1 maintains small, dispersed medullary islets.

**A****B**

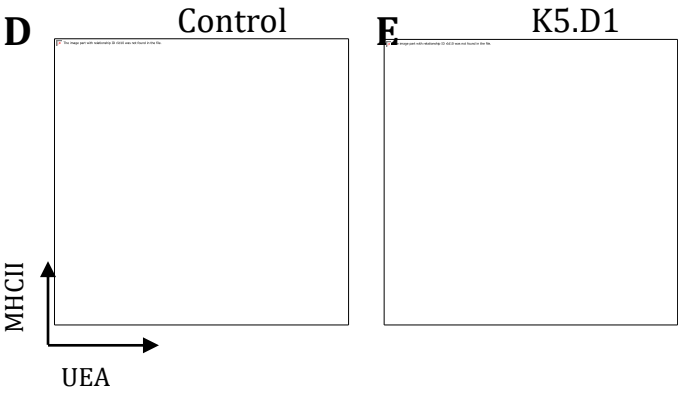
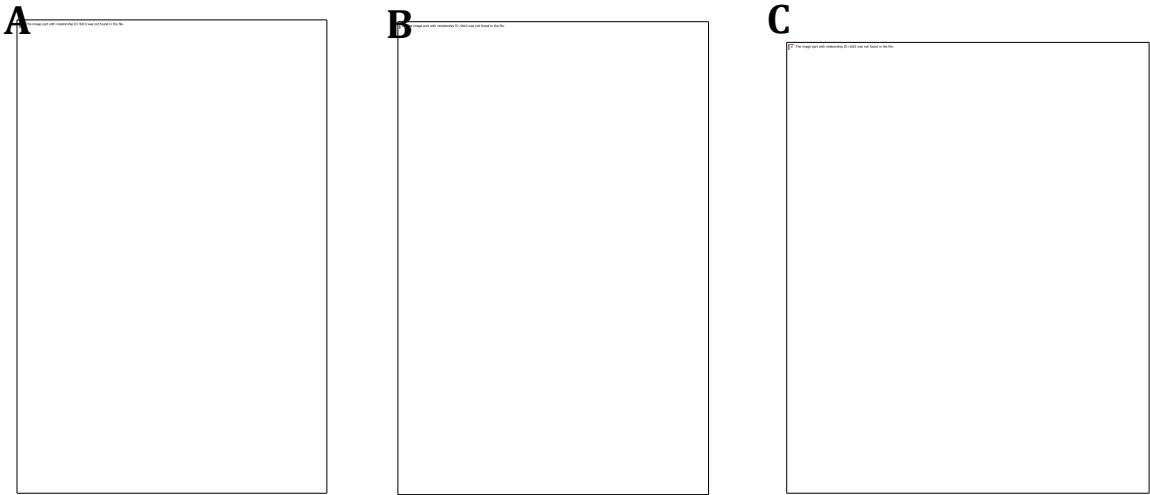
**Figure 8: The K5.D1 adult thymus maintains a perinatal-like localization of TEC subsets**

Representative fluorescent IHC stained sections of (A) P3 WT and K5.D1 thymuses and (B) 6-week WT and K5.D1 Thymuses. K8+K5+K14<sup>-</sup> TECs are widespread in the P3 WT (top of A) and K5.D1 (bottom of A) thymus. K8+K5+K14<sup>-</sup> TECs become mostly restricted to the CMJ in the WT adult thymus (top of B), but remain abundant in the adult K5.D1 thymus cortex (bottom of B). (left of A and B) sections co-stained for K8, K5, K14. (right of A and B) K8 signal removed to enhance visualization of K5+K14<sup>-</sup> TEC.

compartment maintains this cellularity throughout the transition (Fig 9B), but the mTEC compartment rapidly expands until P7, when it shifts to a program of homeostasis (Fig 9A). The K5.D1 thymus replicates the growth pattern of the WT thymus in both the mTEC and cTEC compartments until P7-P10. After P7, the K5.D1 mTEC compartment maintains an exponential growth (Fig 9A). The K5.D1 cTEC compartment remains homeostatic until P10, when it begins its own exponential growth (Fig 9B). These exponential growths of the mTEC and cTEC compartments shift the composition of the post P10 K5.D1 thymus' TEC compartment, eventually returning it to the roughly equal contribution of the cTEC and mTEC compartments seen at birth (Fig 9C).

### **3.4 A phenotypically immature, cycling TEC subset is selectively expanded in the juvenile (P28) K5.D1 thymus**

The conventional method of classifying TEC subsets based on their flow cytometric profiles of surface markers reveals 4 populations. MHCII levels are higher on mature compared to immature cTECs and mTECs (55) (Fig 9D,E). mTECs can be distinguished from cTECs by binding of the lectin UEA-1 binds (Fig 9D,E). The cTEC and mTEC subsets identified by these conventional markers are heterogeneous. This heterogeneity is particularly marked in the K5.D1 thymus where there is a shift in the UEA-1 binding and MHCII expression which prevents discrete populations from being easily identified (Fig 9E). The decrease in expression of MHCII shows that the TECs in the adult K5.D1 thymus are generally less mature than those of the WT, while the decrease in affinity for UEA-1 indicates that the mTECs are less differentiated as well. This decreased maturity and differentiation supports our model, which predicts that the K5.D1 will have decreased terminal differentiation in addition to its increased proliferation. Because of these difficulties, a strategy that provides finer definition of TEC subsets is needed. We found that plotting UEA-1 against Sca-1 gives 5 distinct subsets



MHCII

UEA

**Figure 9: Both mTEC and cTEC subsets are expanded in the K5.D1 thymus.**

(A, B) Representative dot plots of FACs analysis of canonical TEC subsets at P28 in (A) WT and (B) K5.D1 thymuses. Canonical subsets are mature mTECs (MHCII<sup>hi</sup> UEA-1+), immature mTECs (MHCII<sup>lo</sup> UEA-1+), mature cTECs (MHCII<sup>hi</sup> UEA-1-), and immature cTECs (MHCII<sup>lo</sup> UEA-1-). (C, D) Cellularity of total mTEC (C) and cTEC (D) populations throughout the perinatal to juvenile transition. (E) Ratio of percentages of mTECs to cTECs across the perinatal to Juvenile transition. N-value of at least 4 mice per time point and genotype. \*P<0.05, \*\*P<0.01, \*\*\*P< 0.0001, and \*\*\*\*P< 0.00001 using an unpaired two-tailed Student T test.

in the adult WT thymus, which we designate TEC1 – 5 (Fig 10A). The TEC2 subset is a minor population in the WT adult thymus, but is highly enriched in the K5.D1 adult thymus (Fig 10A,B).

In order to determine when the TEC2 subset becomes enriched in the K5.D1 thymus, we conducted FACS analysis of WT and K5.D1 thymuses from a late embryonic stage (E17.5) to the juvenile stage (P28), covering the entirety of the perinatal to juvenile transition. An increased frequency of the TEC2 subset in K5.D1 compared to WT TECs was found to occur by P7 (Fig 10C,D). P7 is the same timepoint at which K5.D1 TEC cellularity diverges from that of the WT (Fig 3B). While the TEC2 subset is heterogeneous as shown, for example by the wide range of UEA-binding levels, the majority of these cells express low levels of MHCII and high levels of CD24 (data not shown) indicating that they are likely to be immature TECs. The immature phenotype and increased frequency of the TEC2 subset suggests that proliferating TEC progenitor cells may be preferentially expanded in the K5.D1 thymus. This concept would be consistent with previous studies showing that RB inactivation increases the frequency of precursor cells in several other tissues (56).

If the TEC2 subset contains a proliferating precursor population, such as transit amplifying cells, we would expect a high frequency of proliferating cells in this subset. We quantified the proportion of Ki67+ in each of the five TEC subsets in WT and K5.D1 thymuses across the perinatal to juvenile transition (Fig 11A). In order to focus on the major findings in this large data set, we calculated the ratio of Ki67+ cells in K5.D1 versus WT for each of the TEC1 – 5 subsets. The ratio for TEC4 and TEC5 was unchanged across the transition, so only TEC1 – 3 are shown (Fig11B). At E17.5 and shortly after birth, the ratio was ~1 for all subsets (Fig 11). This early equivalency between the K5.D1 and WT fits our model that in the early perinatal stage TEC proliferation is RB independent. Starting at day 3 the TEC2 population is selectively

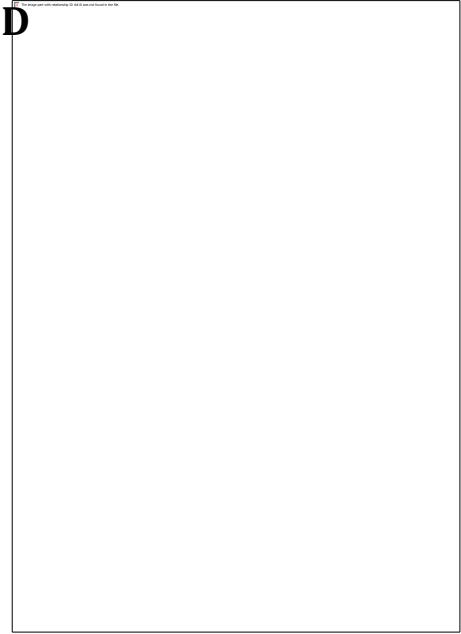
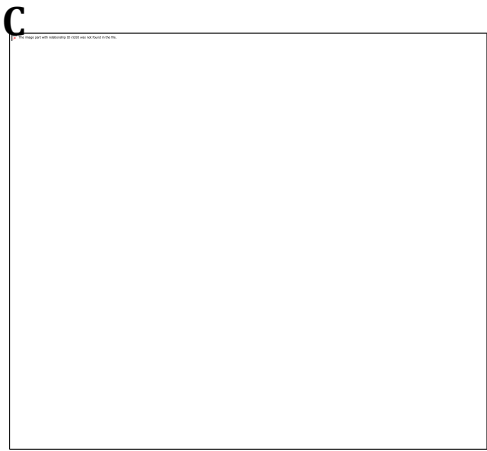
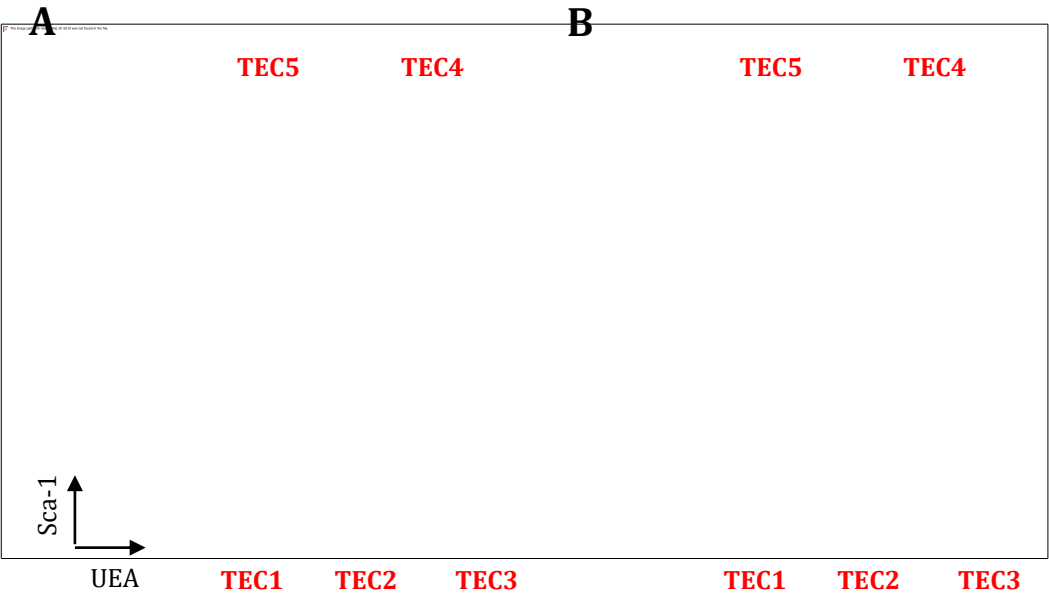




**Figure 10: A novel UEA-1<sup>int</sup> Sca-1- TEC subset is enriched in the K5.D1 thymus compared to WT thymus.**

FACS plots of EpCAM<sup>+</sup> CD45<sup>-</sup> TEC subsets defined by Sca1 and UEA in WT (A) and K5.D1 (B) 4-week-old thymus. TEC1-TEC5 subsets are labeled in red. (C,D)

Percentage (C) and cellularity (D) of TEC2 in WT (blue) and K5.D1 (red) thymus across the perinatal to juvenile transition. N-value of at least 4 mice per time point and genotype. \*P<0.05, \*\*P<0.01, \*\*\*P< 0.0001, and \*\*\*\*P< 0.00001 using an unpaired two-tailed Student T test.

enriched for proliferating cells (Fig 11). At day 14, the TEC1 subset also becomes enriched for proliferating cells (Fig 11), potentially indicating that the TEC2 population is preferentially enriched for cTEC dedicated progenitors.

Our temporal map of the perinatal WT thymus shows that its composition, localization, and structure change rapidly and continually throughout the perinatal to juvenile transition (Fig 12A,C). The results also demonstrate that K5.D1 TECs maintain perinatal-like phenotypic and proliferative characteristics throughout the perinatal to juvenile transition and into adulthood (Fig 12B,D). This maintenance of perinatal-like characteristics supports our working model that early perinatal TECs are primed for proliferation, possibly due to constitutive monophosphorylation of RB, but are primarily programmed for terminal differentiation after P7-P10. Additionally, we identified a novel TEC subset that is likely to contain cells with progenitor activity based on phenotypic and proliferative characteristics.

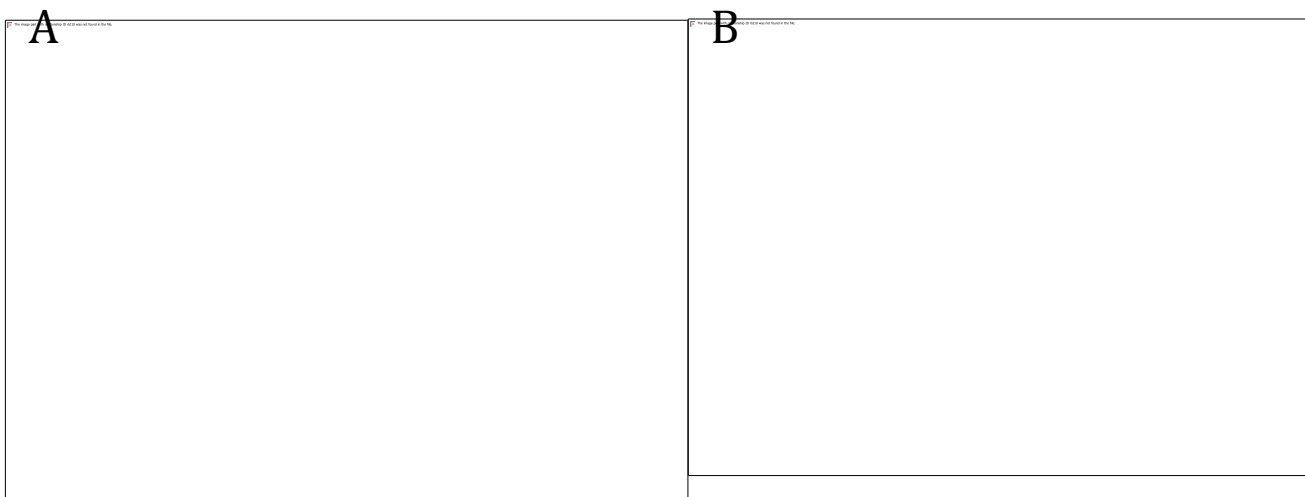


**Figure 11: K5.D1 TEC2 cells are enriched in cycling cells compared to WT TEC2 cells**

(A) Percentage of proliferating cells in WT TEC1-3 populations. (B) Ratio of percentage of proliferating TECs in K5.D1 compared to WT thymuses for TEC1-3 at indicated time points. N-value of at least 4 mice per time point and genotype. N-value of at least 2 mice per time point and genotype.

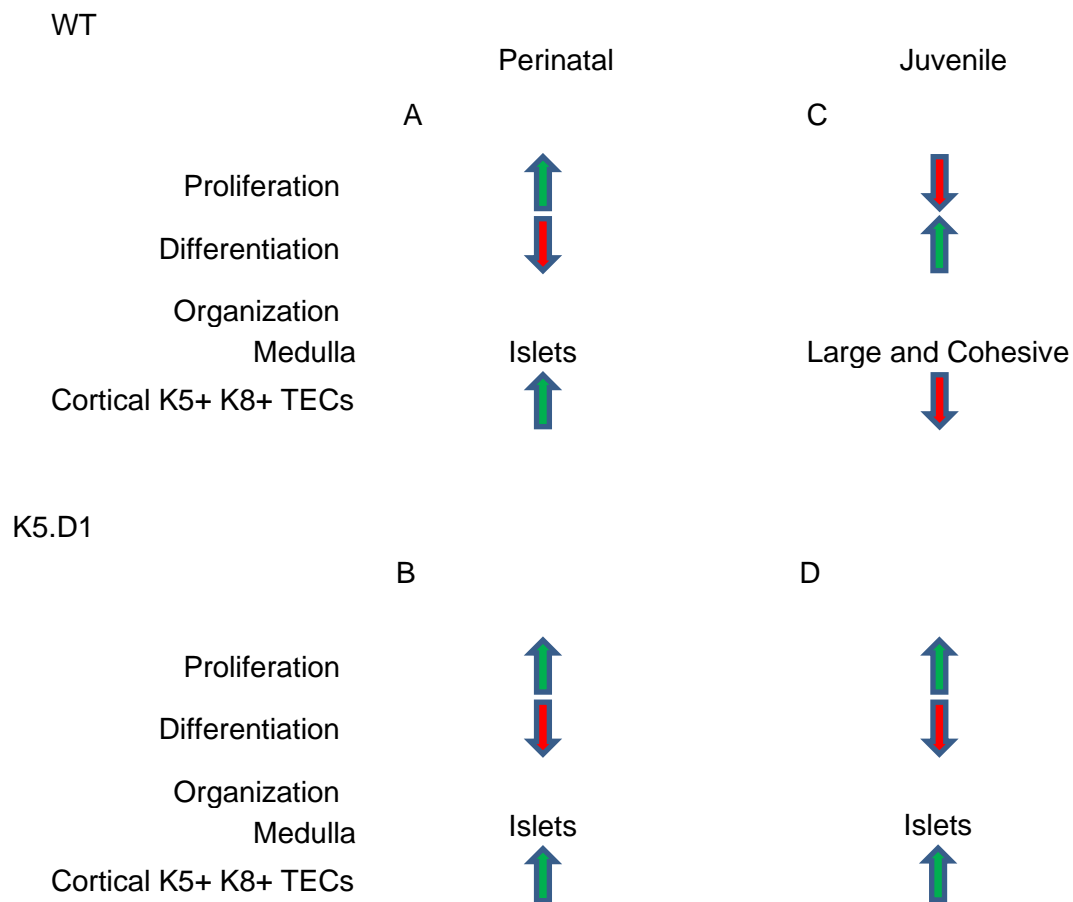


**Figure 12: Summary of results.**

(A & B) In both WT and K5.D1 mice, the perinatal TEC compartment is marked by a high rate of proliferation, incomplete differentiation, small and frequent medullary islets, and widespread K5+ K8+ cortical TECS. (C) By the juvenile stage, the proliferation of WT TECs has decreased and cTEC and mTEC differentiation is complete. The juvenile thymic medulla is large and cohesive, and there are few K5+ K8+ cortical TECs. (D) The juvenile K5.D1 TEC compartment maintains, proliferation, differentiation and organizational features that mimic those of the perinatal TEC compartment.

## 4 Discussion

### 4.1 A temporal map of changes in the TEC compartment during the perinatal to juvenile transition

The results of this investigation show dramatic changes in the cellularity, composition, localization, and proliferation of cortical and medullary TECs during the perinatal to juvenile transition. An earlier study showed that total thymus cellularity increased throughout the perinatal period, peaking by P28 and entering involution between 8 and 10 weeks with the TEC compartment displaying a similar pattern (38). However, there was no distinction made between cTECs and mTECs, and only a short period of the perinatal stage was measured. Additionally, the data from several different time points were combined into a single data point. Our analyses were performed at multiple time points during the perinatal period to create a detailed temporal map of how cellularity and other parameters change in both cTECs and mTECs throughout the perinatal to juvenile transition.

These data demonstrate that the transition from rapid expansion of thymus cellularity to relative homeostasis occurs by P14. Because the thymus is about 98% thymocytes, this transition in total thymus cellularity primarily represents a shift in the growth of the thymocyte compartment. Interestingly, the TEC compartment's growth slows roughly a week earlier, by P7. These results suggest that the increase in thymocytes relies on expansion of the TEC compartment, which is consistent with the notion that TECs provide required niches for thymocyte progenitors (4, 57, 58).

The stages of T cell development have been extensively studied (12). Hematopoietic seeding progenitors are attracted to the thymus by chemokines including CCL19, CCL21, and CCL25 (1-3). These signals specifically attract hematopoietic progenitors to the blood vessels at the CMJ where they enter the thymus. The earliest intrathymic thymocyte progenitors, ETPs, depend on signals from microenvironmental

niches to promote their survival and commitment to the T cell lineage (4, 5). Cortical TECs provide a number of these signals such as IL-7, Notch ligands, and Kit ligand (10, 11). One would predict that as the number of cTECs increases during the early perinatal period in the wildtype thymus, there would be an increased number of niches that support ETP expansion and maturation. Because all stages of thymocyte development begin with ETPs this would be expected to increase the number of thymocytes at later stages as well. When TEC expansion shifts to homeostasis, the number of ETP niches may stabilize, which would in turn stabilize thymocyte numbers. Our temporal map of TEC and thymocyte cellularity supports these expectations.

We also analyzed sex specific growth trends of the perinatal thymus. There are sex specific differences seen in the involuting thymus, with the thymuses of female mice involuting slower than those of males (51). Additionally, castration of male mice rescues the involuting thymus (51). This implicates sex specific hormones as one factor in regulating involution. Because the perinatal to juvenile transition occurs before sexual maturity, we did not expect a sex specific difference in thymus growth. Our data does indeed show that thymus growth and TEC expansion are similar in males and females during the perinatal period.

Our data also show that there are numerous differences in the composition and structure of the TEC compartment between the perinatal and juvenile timepoints. Of particular interest is the increased frequency in the perinatal thymus of the TEC subset that costains for K8 and K5. This population has been implicated as an mTEC precursor population (31), which could indicate that the perinatal thymus has a greater progenitor potential than the juvenile. Additionally, the relative proportion of mTECs to cTECs shifts throughout the perinatal to juvenile transition. While there are roughly equivalent numbers of cTECs and mTECs until day 3, by day 28 there are nearly 8-fold more mTECs than cTECs. Additional experiments would be needed to investigate the causes



of this preferential enrichment for mTECs, but it conforms to the notion that the perinatal thymus expands rapidly to fill the lymphopenic periphery with functioning T cells. The expansion would start with the early emigration of TSPs which would differentiate following the thymocyte development pathway and proliferating in the cortex. It would be several days before these initial waves of thymocytes expressed a functioning  $\alpha\beta$ TCR to enter the medulla. Without a large population of single positive thymocytes to provide the necessary cross talk signals, the mTECs would be unable to proliferate and differentiate.

In addition to changes in the cellularity and composition of the TEC compartment, TEC proliferation changes across the transition. In the late fetal stage and immediately after birth, 30-40% of TECs are actively cycling cells. This number drops dramatically to just ~15% of TECs by P3 and remains low throughout the transition. It is important to note that the reduction in actively cycling cells, as indicated by Ki67 staining, occurs prior to the reduction in TEC compartment growth at day 7 and the plateauing of thymus growth seen at P10-P14. This suggests TEC proliferation is a factor in regulating the growth of the thymus.

#### **4.2 The Cyclin D1-RB-E2F pathway regulates the perinatal to juvenile transition in proliferation**

Our previously published reports (43-45) showed inhibition of RB, whether by overexpression of Cyclin D1 or deletion of the RB family, in TECs maintained a proliferative program in the thymus throughout life. However, the earlier studies did not determine how early growth of the K5.D1 thymus exceeded that of the WT thymus. Our data revealed that disruption of RB-mediated regulation of proliferation affected the growth of the thymus and TEC compartment only after P14 and P3 respectively. The lack of a phenotype in the early perinatal stage in K5.D1 mice led us to develop a working model in which RB in TECs is constitutively monophosphorylated until ~P7. In

the model RB is primarily unphosphorylated at later stages. This predicts that the TECs in the early perinatal stage are primed for hyperphosphorylation of RB, which leads to s-phase entry and continued proliferation. Additionally, after the transition at P7-P14 the change to primarily monophosphorylated RB in TECs would lead to increased terminal differentiation and decreased proliferation.

#### **4.3 Identification of a putative TEC progenitor population**

In addition to providing the basis for our working model of the mechanism regulating the perinatal to juvenile transition, the K5.D1 mouse model also aided in the identification of a novel TEC subset. The canonical method of identifying cTEC and mTEC subsets via flow cytometric analysis identifies four TEC subsets based on levels of MHCII expression, and binding of the UEA-1 lectin or expression of the cell surface marker Ly51 (55, 59). The subsets identified via this method are extremely heterogeneous in the WT as seen, for example, by their wide range of affinity for UEA-1. Additionally, a downward shift in affinity for UEA-1 and expression of MHCII on K5.D1 TECs makes accurate identification of these subsets even less clear-cut as the TECs exhibit a block in differentiation. We identified a new method of subsetting TECs by investigating UEA-1 binding and Sca-1 expression. Although the populations shown by this method are also heterogeneous, it reveals a novel UEA-1<sup>int</sup> Sca-1<sup>+</sup> TEC2 subset that is enriched in the K5.D1 TEC compartment after P3. This subset contains TECs with low expression of MHCII and CD24 indicating that it is an immature population of TECs. The TEC2 subset is expanded in the K5.D1 thymus after P3 and maintains perinatal-like proliferation at P3. Since both cTECs and mTECs are expanded in the K5.D1 thymus, and the K5.D1 is predicted to have a block in terminal differentiation, the TEC2 subset may contain precursor cells for both cTECs and mTECs. The high frequency of proliferating cells in the K5.D1 TEC2 subset suggests that it contains transit amplifying

cells that generate cTECs and mTECs. If this subset does contain a precursor population, RB regulation of its proliferation would be consistent with other reports showing RB-mediated regulation of cell cycle exit and differentiation in precursor cells of other tissues such as skin and the adult hematopoietic system (56). This putative precursor population could contain a population that is bipotent for both cTECs and mTECs, cTEC and/or mTEC lineage committed precursors, or a mixture of both.

#### **4.4 Future Studies**

In this study, we have created an in-depth temporal map of changes in the TEC compartment throughout the perinatal to juvenile transition. We have used this map to identify a potential pathway regulating the transition. In the future, changes in the TEC compartment throughout the perinatal period can be integrated with data on T cell development to reveal how perinatal TECs contribute to the unique functions of perinatal T cells. There are also still gaps in our understanding of the regulation of the perinatal to juvenile transition. It is currently unknown if the TEC2 subset functions as a precursor population. In vitro colony forming assays and in vivo reaggregate thymic organ culture experiments have both been used to investigate TEC precursor activity. Using either of these two methods, we can identify the contribution of specific TEC subsets to each TEC compartment. Doing so with a range of input concentrations of our putative progenitor subset allows us to use a limiting dilution statistical analysis to calculate the frequency and number of cTEC and mTEC precursor cells in the population.

### Bibliography

1. Lind, E. F., S. E. Prockop, H. E. Porritt, and H. T. Petrie. 2001. Mapping precursor movement through the postnatal thymus reveals specific microenvironments supporting defined stages of early lymphoid development. *J Exp Med* 194: 127-134.
2. Bhandoola, A., H. von Boehmer, H. T. Petrie, and J. C. Zuniga-Pflucker. 2007. Commitment and developmental potential of extrathymic and intrathymic T cell precursors: plenty to choose from. *Immunity* 26: 678-689.
3. Koch, U., and F. Radtke. 2011. Mechanisms of T cell development and transformation. *Annu Rev Cell Dev Biol* 27: 539-562.
4. Zietara, N., M. Lyszkiewicz, J. Puchalka, K. Witzlau, A. Reinhardt, R. Forster, O. Pabst, I. Prinz, and A. Krueger. 2015. Multicongenic fate mapping quantification of dynamics of thymus colonization. *J Exp Med* 212: 1589-1601.
5. Goldschneider, I. 2006. Cyclical mobilization and gated importation of thymocyte progenitors in the adult mouse: evidence for a thymus-bone marrow feedback loop. *Immunological Reviews* 209: 58-75.
6. Manley, N. R., E. R. Richie, C. C. Blackburn, B. G. Condie, and J. Sage. 2011. Structure and function of the thymic microenvironment. *Frontiers in Bioscience* 16: 2461-2477.
7. Shortman, K., and L. Wu. 1996. Early T Lymphocyte Progenitors. *Annual Review of Immunology* 14: 29-47.
8. Bell, J. J., and A. Bhandoola. 2008. The earliest thymic progenitors for T cells possess myeloid lineage potential. *Nature* 452: 764-767.
9. Schmitt, T. M., M. Ciofani, H. T. Petrie, and J. C. Zuniga-Pflucker. 2004. Maintenance of T cell specification and differentiation requires recurrent notch receptor-ligand interactions. *J Exp Med* 200: 469-479.

10. Koch, U., E. Fiorini, R. Benedito, V. Besseyrias, K. Schuster-Gossler, M. Pierres, N. R. Manley, A. Duarte, H. R. Macdonald, and F. Radtke. 2008. Delta-like 4 is the essential, nonredundant ligand for Notch1 during thymic T cell lineage commitment. *J Exp Med* 205: 2515-2523.
11. Hozumi, K., C. Mailhos, N. Negishi, K. Hirano, T. Yahata, K. Ando, S. Zuklys, G. A. Hollander, D. T. Shima, and S. Habu. 2008. Delta-like 4 is indispensable in thymic environment specific for T cell development. *J Exp Med* 205: 2507-2513.
12. Shah, D. K., and J. C. Zuniga-Pflucker. 2014. An overview of the intrathymic intricacies of T cell development. *J Immunol* 192: 4017-4023.
13. Feyerabend, T. B., G. Terszowski, A. Tietz, C. Blum, H. Luche, A. Gossler, N. W. Gale, F. Radtke, H. J. Fehling, and H. R. Rodewald. 2009. Deletion of Notch1 converts pro-T cells to dendritic cells and promotes thymic B cells by cell-extrinsic and cell-intrinsic mechanisms. *Immunity* 30: 67-79.
14. Wada, H., K. Masuda, R. Satoh, K. Kakugawa, T. Ikawa, Y. Katsura, and H. Kawamoto. 2008. Adult T-cell progenitors retain myeloid potential. *Nature* 452: 768-772.
15. Wilson, A., H. R. MacDonald, and F. Radtke. 2001. Notch 1-deficient common lymphoid precursors adopt a B cell fate in the thymus. *J Exp Med* 194: 1003-1012.
16. Petrie, H. T., and J. C. Zuniga-Pflucker. 2007. Zoned out: functional mapping of stromal signaling microenvironments in the thymus. *Annu Rev Immunol* 25: 649-679.
17. Michie, A. M., and J. C. Zúñiga-Pflücker. 2002. Regulation of thymocyte differentiation: pre-TCR signals and  $\beta$ -selection. *Seminars in Immunology* 14: 311-323.

18. von Boehmer, H. 2005. Unique features of the pre-T-cell receptor  $\alpha$ -chain: not just a surrogate. *Nature Reviews Immunology* 5: 571-577.
19. Pénit, C., B. Lucas, and F. Vasseur. 1995. Cell expansion and growth arrest phases during the transition from precursor (CD4-8-) to immature (CD4+8+) thymocytes in normal and genetically modified mice. *The Journal of Immunology* 154: 5103-5113.
20. Klein, L., M. Hinterberger, G. Wirnsberger, and B. Kyewski. 2009. Antigen presentation in the thymus for positive selection and central tolerance induction. *Nat Rev Immunol* 9: 833-844.
21. Klein, L., B. Kyewski, P. M. Allen, and K. A. Hogquist. 2014. Positive and negative selection of the T cell repertoire: what thymocytes see (and don't see). *Nat Rev Immunol* 14: 377-391.
22. Kurobe, H., C. Liu, T. Ueno, F. Saito, I. Ohigashi, N. Seach, R. Arakaki, Y. Hayashi, T. Kitagawa, M. Lipp, R. L. Boyd, and Y. Takahama. 2006. CCR7-dependent cortex-to-medulla migration of positively selected thymocytes is essential for establishing central tolerance. *Immunity* 24: 165-177.
23. Kyewski, B., and L. Klein. 2006. A central role for central tolerance. *Annu Rev Immunol* 24: 571-606.
24. Koble, C., and B. Kyewski. 2009. The thymic medulla: a unique microenvironment for intercellular self-antigen transfer. *J Exp Med* 206: 1505-1513.
25. Coquet, J. M., J. C. Ribot, N. Babala, S. Middendorp, G. van der Horst, Y. Xiao, J. F. Neves, D. Fonseca-Pereira, H. Jacobs, D. J. Pennington, B. Silva-Santos, and J. Borst. 2013. Epithelial and dendritic cells in the thymic medulla promote CD4+Foxp3+ regulatory T cell development via the CD27-CD70 pathway. *J Exp Med* 210: 715-728.

26. Shevach, E. M. 2009. Mechanisms of foxp3+ T regulatory cell-mediated suppression. *Immunity* 30: 636-645.
27. Zachariah, M. A., and J. G. Cyster. 2010. Neural Crest–Derived Pericytes Promote Egress of Mature Thymocytes at the Corticomedullary Junction. *Science* 328: 1129-1135.
28. Rossi, S. W., W. E. Jenkinson, G. Anderson, and E. J. Jenkinson. 2006. Clonal analysis reveals a common progenitor for thymic cortical and medullary epithelium. *Nature* 441: 988-991.
29. Bennett, A. R., A. Farley, N. F. Blair, J. Gordon, L. Sharp, and C. C. Blackburn. 2002. Identification and Characterization of Thymic Epithelial Progenitor Cells. *Immunity* 16: 803-814.
30. Ulyanchenko, S., K. E. O'Neill, T. Medley, A. M. Farley, H. J. Vaidya, A. M. Cook, N. F. Blair, and C. C. Blackburn. 2016. Identification of a Bipotent Epithelial Progenitor Population in the Adult Thymus. *Cell Rep* 14: 2819-2832.
31. Wong, K., N. L. Lister, M. Barsanti, J. M. Lim, M. V. Hammett, D. M. Khong, C. Siatskas, D. H. Gray, R. L. Boyd, and A. P. Chidgey. 2014. Multilineage potential and self-renewal define an epithelial progenitor cell population in the adult thymus. *Cell Rep* 8: 1198-1209.
32. Hamazaki, Y., M. Sekai, and N. Minato. 2016. Medullary thymic epithelial stem cells: role in thymic epithelial cell maintenance and thymic involution. *Immunological Reviews* 271: 38-55.
33. Hamazaki, Y., H. Fujita, T. Kobayashi, Y. Choi, H. S. Scott, M. Matsumoto, and N. Minato. 2007. Medullary thymic epithelial cells expressing Aire represent a unique lineage derived from cells expressing claudin. *Nat Immunol* 8: 304-311.

34. Xing, Y., S. C. Jameson, and K. A. Hogquist. 2013. Thymoproteasome subunit- $\beta$ 5T generates peptide-MHC complexes specialized for positive selection. *Proceedings of the National Academy of Sciences* 110: 6979-6984.
35. Anderson, M. S., E. S. Venanzi, L. Klein, Z. Chen, S. P. Berzins, S. J. Turley, H. von Boehmer, R. Bronson, A. Dierich, C. Benoist, and D. Mathis. 2002. Projection of an Immunological Self Shadow Within the Thymus by the Aire Protein. *Science* 298: 1395-1401.
36. Yano, M., N. Kuroda, H. Han, M. Meguro-Horike, Y. Nishikawa, H. Kiyonari, K. Maemura, Y. Yanagawa, K. Obata, S. Takahashi, T. Ikawa, R. Satoh, H. Kawamoto, Y. Mouri, and M. Matsumoto. 2008. Aire controls the differentiation program of thymic epithelial cells in the medulla for the establishment of self-tolerance. *J Exp Med* 205: 2827-2838.
37. Stritesky, G. L., Y. Xing, J. R. Erickson, L. A. Kalekar, X. Wang, D. L. Mueller, S. C. Jameson, and K. A. Hogquist. 2013. Murine thymic selection quantified using a unique method to capture deleted T cells. *Proceedings of the National Academy of Sciences* 110: 4679-4684.
38. Gray, D. H., N. Seach, T. Ueno, M. K. Milton, A. Liston, A. M. Lew, C. C. Goodnow, and R. L. Boyd. 2006. Developmental kinetics, turnover, and stimulatory capacity of thymic epithelial cells. *Blood* 108: 3777-3785.
39. Dick, F. A., and S. M. Rubin. 2013. Molecular mechanisms underlying RB protein function. *Nat Rev Mol Cell Biol* 14: 297-306.
40. Dyson, N. J. 2016. RB1: a prototype tumor suppressor and an enigma. *Genes & Development* 30: 1492-1502.
41. Knudsen, K. E. 2006. The cyclin D1b splice variant: an old oncogene learns new tricks. *Cell Div* 1: 15.



42. Sanidas, I., R. Morris, K. A. Fella, P. H. Rumde, M. Boukhali, E. C. Tai, D. T. Ting, M. S. Lawrence, W. Haas, and N. J. Dyson. 2019. A Code of Mono-phosphorylation Modulates the Function of RB. *Mol Cell* 73: 985-1000 e1006.
43. Klug, D. B., E. Crouch, C. Carter, L. Coghlan, C. J. Conti, and E. R. Richie. 2000. Transgenic expression of cyclin D1 in thymic epithelial precursors promotes epithelial and T cell development. *J Immunol* 164: 1881-1888.
44. Robles, A. I., F. Larcher, R. B. Whalin, R. Murillas, E. Richie, I. B. Gimenez-Conti, J. L. Jorcano, and C. J. Conti. 1996. Expression of cyclin D1 in epithelial tissues of transgenic mice results in epidermal hyperproliferation and severe thymic hyperplasia. *Proceedings of the National Academy of Sciences* 93: 7634-7638.
45. Garfin, P. M., D. Min, J. L. Bryson, T. Serwold, B. Edris, C. C. Blackburn, E. R. Richie, K. I. Weinberg, N. R. Manley, J. Sage, and P. Viatour. 2013. Inactivation of the RB family prevents thymus involution and promotes thymic function by direct control of Foxn1 expression. *J Exp Med* 210: 1087-1097.
46. Opiela, S. J., T. Koru-Sengul, and B. Adkins. 2009. Murine neonatal recent thymic emigrants are phenotypically and functionally distinct from adult recent thymic emigrants. *Blood* 113: 5635-5643.
47. Smith, N. L., R. K. Patel, A. Reynaldi, J. K. Grenier, J. Wang, N. B. Watson, K. Nzingha, K. J. Yee Mon, S. A. Peng, A. Grimson, M. P. Davenport, and B. D. Rudd. 2018. Developmental Origin Governs CD8(+) T Cell Fate Decisions during Infection. *Cell* 174: 117-130 e114.
48. Yang, S., N. Fujikado, D. Kolodin, C. Benoist, and D. Mathis. 2015. Immune tolerance. Regulatory T cells generated early in life play a distinct role in maintaining self-tolerance. *Science* 348: 589-594.

49. Tuncel, J., C. Benoist, and D. Mathis. 2019. T cell anergy in perinatal mice is promoted by T reg cells and prevented by IL-33. *J Exp Med* 216: 1328-1344.
50. Scharschmidt, T. C., K. S. Vasquez, H. A. Truong, S. V. Gearty, M. L. Pauli, A. Nosbaum, I. K. Gratz, M. Otto, J. J. Moon, J. Liese, A. K. Abbas, M. A. Fischbach, and M. D. Rosenblum. 2015. A Wave of Regulatory T Cells into Neonatal Skin Mediates Tolerance to Commensal Microbes. *Immunity* 43: 1011-1021.
51. Gui, J., L. M. Mustachio, D.-M. Su, and R. W. Craig. 2012. Thymus Size and Age-related Thymic Involution: Early Programming, Sexual Dimorphism, Progenitors and Stroma. *Aging Dis* 3: 280-290.
52. Rodewald, H.-R., S. Paul, C. Haller, H. Bluethmann, and C. Blum. 2001. Thymus medulla consisting of epithelial islets each derived from a single progenitor. *Nature* 414: 763-768.
53. Klug, D. B., C. Carter, E. Crouch, D. Roop, C. J. Conti, and E. R. Richie. 1998. Interdependence of cortical thymic epithelial cell differentiation and T-lineage commitment. *Proceedings of the National Academy of Sciences* 95: 11822-11827.
54. Onder, L., V. Nindl, E. Scandella, Q. Chai, H.-W. Cheng, S. Caviezel-Firner, M. Novkovic, D. Bomze, R. Maier, F. Mair, B. Ledermann, B. Becher, A. Waisman, and B. Ludewig. 2015. Alternative NF- $\kappa$ B signaling regulates mTEC differentiation from podoplanin-expressing precursors in the cortico-medullary junction. *European Journal of Immunology* 45: 2218-2231.
55. Abramson, J., and G. Anderson. 2017. Thymic Epithelial Cells. *Annual Review of Immunology* 35: 85-118.
56. Sage, J. 2012. The retinoblastoma tumor suppressor and stem cell biology. *Genes Dev* 26: 1409-1420.

57. Donskoy, E., D. Foss, and I. Goldschneider. 2003. Gated importation of prothymocytes by adult mouse thymus is coordinated with their periodic mobilization from bone marrow. *J Immunol* 171: 3568-3575.
58. Gossens, K., S. Naus, S. Y. Corbel, S. Lin, F. M. Rossi, J. Kast, and H. J. Ziltener. 2009. Thymic progenitor homing and lymphocyte homeostasis are linked via S1P-controlled expression of thymic P-selectin/CCL25. *J Exp Med* 206: 761-778.
59. Anderson, G., and Y. Takahama. 2012. Thymic epithelial cells: working class heroes for T cell development and repertoire selection. *Trends Immunol* 33: 256-263.

### **Vita**

Scott Howard Casey was born in Las Vegas, Nevada, the son of Steve Shannon Casey and Linda Schneider Casey. After completing his degree at The Meadows School, Las Vegas, NV in 2003 he entered Cornell College in Mt. Vernon, Iowa. He received the degree of Bachelor of Arts with a major in biochemistry and molecular biology from Cornell College in June 2014. In July 2015, he entered The University of Texas MD Anderson Cancer Center UTHHealth Graduate School of Biomedical Sciences.

Permanent address:

3950 TX Hwy 71 East,

Apt 714

Bastrop, TX 78602